High-Tech Fidget Spinner: Open-Source 3 Axis Turntable

Anonymous Author(s)

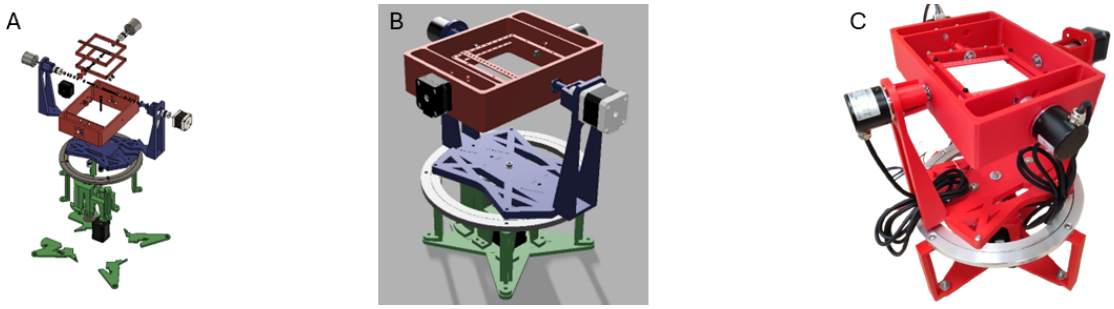

Figure 1: 3-DoF High-Tech Fidget Spinner exploded view (A), rendered model (B) and working prototype (C).

Abstract

This paper presents an unprecedented fully open-source, 3-DoF turntable designed to enable precise characterisation and validation of inertial measurement units (IMUs), for under £500 ($670), which is a fraction of the cost of commercial systems. This design combines 3D-printed mechanical parts, off-the-shelf 3D printer electronics, and custom firmware with a web-based trajectory generator. Users define piecewise motion profiles for roll, pitch, and yaw via a cross-platform GUI; trajectories are saved to MicroSD and executed on a Teensy 4.1-based controller. The system can achieve a mean deviation as small as 0.0075°, and can hold a wide range of different IMU devices within a $100mm \times 100mm$ area using its universal mounting fixture. All CAD files (STL/3MF/Fusion 360), electronics schematics, firmware source code, and configuration tools are freely available under the GNU GPLv3 license. This platform lowers the barrier to rigorous IMU testing for researchers, educators, and makers without six-figure budgets, which is what it would cost to purchase a commercial solution.

CCS Concepts

• **Hardware** → *Semi-formal verification*; *Semi-formal verification*; PCB design and layout.

Keywords

3D Design, Custom Firwmare, IMU, CAD, PCB Design

ACM Reference Format:

Anonymous Author(s). 2018. High-Tech Fidget Spinner: Open-Source 3 Axis Turntable. In *Proceedings of Make sure to enter the correct conference title from your rights confirmation email (Conference acronym 'XX)*. ACM, New York, NY, USA, 7 pages. https://doi.org/XXXXXXX.XXXXXXX

Conference acronym 'XX, Woodstock, NY

ACM ISBN 978-1-4503-XXXX-X/2018/06
https://doi.org/XXXXXXX.XXXXXXX

1 Introduction

1.1 Motivation and Context

Wearable motion tracking systems increasingly rely on inertial measurement units (IMU sensors) to capture biomechanical kinematics live in the field, outside of laboratory settings. They are a "cost-effective way to measure biomechanical and physiological data... compared to laboratory gold standards" according to Arlotti et al. [1]. The total addressable market (TAM) for wearables grew by 23.1% from 2020 to 2021, reaching $10.28 billion [19], with 84% of devices used for exploring upper extremity musculoskeletal conditions containing IMU sensors [30].

Conventional IMU validation against optical motion capture systems is prone to marker misalignment, frame rate limitations, and soft tissue artifact (STA) in biomechanical contexts [20], producing a reported error of up to ±42°using a VR-based system [29]. Mechanical rigs with rotary encoders (turntables) offer a more accurate ground truth with a relative error below 9% as reported by Jia et al. [17]. Such IMU turntables are commercially available, but they are costly in the 5 to 6-figure USD range with proprietary firmware as shown in Table 1. This causes inconsistent data comparisons across different studies, and high costs hinder reproducible research.

1.2 Contributions

To address the aforementioned challenges, this paper presents the "High-Tech Fidget Spinner". It is a fully documented, vendor-agnostic and low-cost open-source turntable for IMU characterisation and data validation. This project contributes:

- **Hardware and Mechanical Design:** A modular 3-DOF gimbal built from 3D-printed PLA parts and off-the-shelf 3D printer components that can execute pre-set trajectories and universally mount any device containing an IMU sensor.
- **Electronics and Control:** A control system based on a Teensy 4.1 microcontroller with three TMC2209 drivers and rotary encoders to execute a pre-set trajectory and capture the ground truth.
- **Firmware and Software:** Custom C++ firmware reads binary trajectory files from a MicroSD card, and a Python web app enables intuitive generation of piecewise X/Y/Z profiles.

- **Open Ecosystem:** Full CAD files, BoM, schematics, source code, and documentation released under the GNU GPLv3 license.
- **Validated performance:** Customisable and repeatable rotations about 3 axes with sub-degree precision.

2 Related Work

2.1 Commercial and Closed-Source IMU Validation Rigs

In Table 1, there is a range of options with varying degrees of freedom, resolution and sample rate. Often, the costs are not listed; however, the costs of the 3LT400 and 13T300 are publicly available and are in the six-figure USD range. Apart from the JAYEGT turntable, the angular resolution of commercial turntables is at least in the order of magnitude of a thousandth of a degree, with their sampling rates ranging from hundreds of hertz to thousands of hertz.

The JAYEGT turntable is a novelty item, often used for photography. It is not designed to calibrate IMU sensors. Although with such a device, the cost barrier is minimal, it would not be suitable for IMU calibration; Its resolution data and sample rate, amongst other things, are not available.

Table 1: Commercially-available turntables

Model	Cost / USD	DoF	Resolution / °	Sample Rate / Hz
Firepower Control 3LT400 [24]	210, 000.00	3	0.000833	80
Firepower Control 2TS-450[3]	NA	2	0.006	1000
Blue Equator BE-INS2-22D08 [9]	NA	2	0.00139	NA
Firepower Control 1LT300 [25]	180, 000.00	1	0.0001	100
iMAR iTES-PDT07[14]	NA	1	0.00153	NA
iMAR iTURN-2D1-HIL[13]	NA	2	5.56×10^{-6}	1000
iMAR iTURN-3S1[12]	NA	3	0.0002	1000
JAYEGT Motorized Rotating Display Stand[16]	41.90	1	NA	NA

2.2 DIY and Academic IMU Validation Rigs

There are free plans available on the internet for DIY 1 DoF turntable builds [11] [22] [26], and Viera et al. describe the construction of a simple turntable [28].

Some designs available online employ 3D-printed gear mechanisms [11] [22]. Such mechanisms are not suitable for a turntable designed to characterise and validate IMU data due to the non-zero backlash [7].

Other designs [26] [28] employ a direct connection between the rotational actuator shaft and turntable. Under the conditions of a properly fastened connection, the backlash issue with gear transmissions is eliminated. However, the designs do not include any rotary encoders to provide a ground truth to compare the IMU data against.

2.3 Open-Source Hardware in Wearables

Open-source hardware should be findable, accessible, interoperable and reproducible [2]. With commercial solutions, they are findable but not accessible due to their cost, not interoperable due to their proprietary firmware and not reproducible due to companies' intellectual property rights. DIY solutions are often findable, accessible, interoperable with modifications and reproducible, but they are not fit for IMU characterisation and validation.

3 Artifact Overview

3.1 Design Goals

From studying the Related Work, the following design goals were chosen to fill in the gaps identified:

- 3 DoF to provide more functionality than some commercial options.
- Logging synchronous IMU and absolute rotation data to be able to calculate error statistics.
- Fully documented, following the FAIR principles [2] and has a minimal cost.
- 360°of continuous rotation about each rotational axis, like commercial solutions in Table 1.
- A rotational actuation resolution up to 0.05625°to match the maximum possible resolution by Viera et al. [28].
- Bespoke user-defined trajectories for versatility.

3.2 System Architecture

A browser GUI (HTML/CSS/JS frontend, Python/Flask backend) lets users define bespoke piecewise motion profiles and stepper-motor parameters. It discretises each axis's trajectory into timed angle-step binaries, saves them to a MicroSD card, and the Teensy 4.1 controller (with TMC2209 drivers) loads and executes them on the X, Y, and Z steppers. During operation, the controller logs actual angles via rotary encoders, and IMU data can stream over UART, I2C, or SPI — or be logged separately.

3.3 Licensing and Repository

This High-Tech Fidget Spinner is licensed under the GNU GPLv3 which lets the community use the project however they wish, apart from distributing it as closed-source versions. It can be found on GitHub via the following URL:

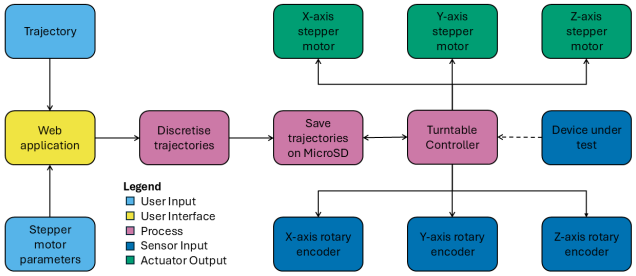

Figure 2: Browser GUI exports user's trajectories as motion binaries to MicroSD, which the artifact executes.

`https://github.com/UpsidedownFalcon/IMU-Turntable`

The README file contains the repository structure; there is a detailed assembly; there is a post-assembly checklist, and a usage guide on the GitHub.

4 Mechanical Design

The High-Tech Fidget Spinner consists of a 3-DOF gimbal structure with motor and sensor mounts. A rotating base provides rotation about the Z axis. On top of the rotating base, two other orthogonal rotation systems are mounted for rotation about the X and Y axes. A direct connection between the stepper motors and rotating body was chosen instead of a mechanism such as gearboxes or pulleys to remove the backlash found in such systems [7]. Bearings and a lazy susan have been used to support each frame of rotation, ensure each frame rotates only about its axis and to ensure that the axes of rotation are orthogonal.

All of the rotational frames and brackets were 3D printed on a Bambulabs X1E 3D printer out of PLA with a 0.2*mm* layer height and 15% infill. The clamping parts for the universal mounting fixture were 3D printed on an Ender 5 out of 85A TPU with a 0.2*mm* layer height and 20% infill.

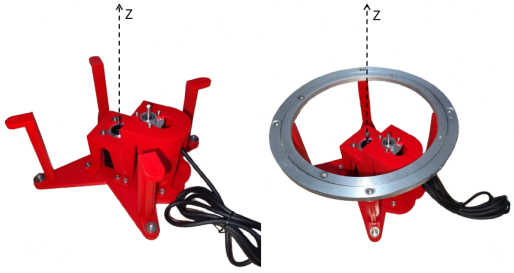

Figure 3: Base frame sub-assembly (left) for rotation about the Z-axis. A lazy susan (right) adds stability to the sub-assemblies mounted on the base.

Figure 3 shows the base sub-assembly with 4 vertical posts; a bracket for the base stepper motor; a bracket for the base rotary encoder and a lazy susan. The vertical posts are mounts for the lazy susan, which provides stability for additonal sub-assemblies mounted on top of the base. The base stepper motor rotates the device under test (DUT) about the Z-axis and the base rotary encoder measures the rotation about the Z-axis. The rotary encoder is connected to the stepper motor via a GT20 timing belt due to their little backlash, as the " backlash is distributed over a full half turn rather than happening immediately on direction change" [23]. Due to practical design considerations of a direct connection between the Z-axis rotary encoder and rotating sub-assemblies on top of the base, the rotary encoder was driven by a timing belt and pulley system rather than a direct drive.

Figure 4: Middle frame sub-assembly for rotation about the Y-axis.

Figure 4 shows the middle sub-assembly with a mount to the lazy susan on the base; stepper motor mount and a rotary encoder mount. It can be mounted to the lazy susan on the base to ensure stable rotation in the X-Y plane, and a stepper motor and rotary encoder can be mounted along the Y-axis. This allows for rotation about the Y-axis and its measurement.

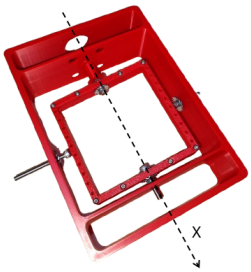

Figure 5: Inner frame sub-assembly for rotation about the X-axis.

Figure 5 shows the inner sub-assembly with a mount for the DUT; stepper motor mount; a rotary encoder mount and a mount to the middle assembly. The mount to the middle assembly is a pair of M5 machine screws which attach to the Y-axis stepper motor and rotary encoder through a set of bearings. The inner assembly can be connected to a stepper motor and rotary encoder to rotate the DUT about the X-axis and measure its rotation. The mount for the DUT forms part of the universal mounting fixture, with its other part being 3D-printed out of TPU.

Figure 1 shows the complete mechanical assembly of the High-Tech Fidget Spinner with a single point of rotation in the middle of the inner frame about three orthogonal axes. Its cost is under £500 ($670).

Figure 6 shows the second half of the universal mounting fixture which is 3D printed out of TPU and attached to the inner frame.

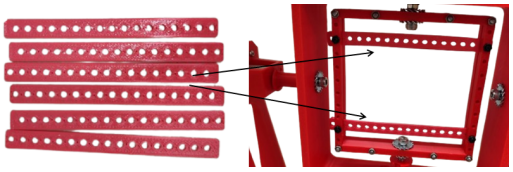

Figure 6: Universal mounting fixture made out of TPU (left) attached to the inner frame (right).

The user can configure how many TPU mounts they need, where to place them and their tension using the holes in the TPU mount and the inner frame. The TPU mount is attached to the inner frame using M3 machine screws.

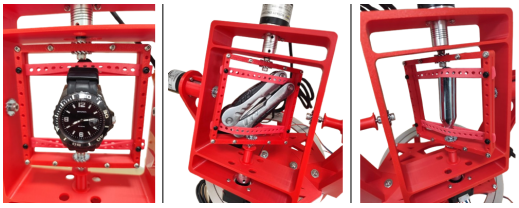

Figure 7: A watch (left), a multitool (middle) and a CO2 canister (right) secured using the universal mounting fixture.

Figure 7 shows the universal mounting fixture securely holding a watch, a multitool and a CO2 canister to demonstrate that it can hold a range of different objects, and hence, a range of IMU devices. The user has flexibility over where and how to place their object for their bespoke application.

5 Electronics and Firmware

5.1 Stepper Motor Selection

5.1.1 Stepper Motors. To meet the rotational requirements of a 3-axis rig with $\geq 360°$range and $\leq 0.05625°$resolution, open-loop stepper motors were selected due to their high native angular precision, ease of control, and widespread availability in open-source hardware ecosystems [5]. Standard stepper motors typically offer step angles of 1.8° (200 steps/rev) or 0.9° (400 steps/rev); combined with microstepping up to 1/256, resolutions as fine as 0.0035° per microstep are attainable without the need for encoders [6]. Stepper drivers such as the TMC2209 interface via simple STEP/DIR signals, eliminating the complexity of feedback control systems used in DC or BLDC motors [27].

5.1.2 Dynamic Torque Modeling. Table 1 shows commercial IMU turntables that have angular accelerations in the order of magnitude of $1000 - 10000°/s^2$. However, Firepower Control's 2TS-450 IMU turntable has an angular acceleration of $300°/s^2$ [3]. To match that angular acceleration of $300°/s^2$ ($\approx$ 5.236 rad/s^2), each axis was modelled as a compound rigid body composed of rotor inertias and the inertia of the IMU payload. The IMU, modelled as a 15.25 mm long, 11.86 g rod, yields a moment of inertia of 1.38×10^{-6} kg $\cdot$ m^2. Detailed models and calculations are explained in the *PRD.md* document on GitHub.

Torque requirements for each axis were computed as follows using a custom Python script, *Stepper_Selection_Model.py*, which can be found on GitHub:

- **X-axis:** $\tau = (2I_{\text{RX}} + I_{\text{IMU}}) \cdot \alpha$
- **Y-axis:** $\tau = \left(\frac{1}{12}(2M_{\text{X}} + M_{\text{IMU}})L^2 + 2I_{\text{RY}}\right) \cdot \alpha$
- **Z-axis:** $\tau = \left(\frac{1}{2}(2M_{\text{X}} + 2M_{\text{Y}} + M_{\text{IMU}})R^2 + 2I_{\text{RZ}}\right) \cdot \alpha$

A safety factor of 10× was applied to each calculated torque to ensure robustness under dynamic loading.

5.1.3 Selected Motors. The custom Python script was used to search and evaluate commercially available stepper motors, filtering for those that meet the required torque, size, and inertia constraints with adequate margin and lead time. The selected models are:

- **X-axis:** Nema 17 42-23
- **Y-axis:** Nema 17 42-38
- **Z-axis:** Nema 17 42-60

Anyone can use *Stepper_Selection_Model.py* to locate suitable stepper motors which they can easily source form their local suppliers.

5.1.4 Microcontroller, Drivers and Rotary Encoders. In order for the High-Tech Fidget Spinner to be as versatile as possible, the user should be able to connect their own IMU sensor to its controller and add to the firmware to log data over any digital communication protocol they choose. Commercial IMU turntables in Table 1 often have CAN bus connectors, which not all data logging devices (for example laptops) have, and there are inconsistent USB ports and protocols between data logging devices. Different data loggers may use different standards such as CAN bus, SDI-12 and MODBUS. Since there is no single data logging standard [10], there may be interoperability and versatility issues if the High-Tech Fidget Spinner depended on one. Hence, the High-Tech Fidget Spinner must be able to independently function, which will require its own onboard storage for saving logged data.

Dynamic current control ensures smooth stepper performance under varying loads, and having the option for the maximum of256-microstep drivers can maximise angular resolution and versatility.

Optical rotary encoders have a greater accuracy and resolution than magnetic rotary encoders [21]. The resolution of an optical rotary encoder can be described by the number of pulses per revolution (PPR), counts per revolution (CPR) or lines per revolution (LPR) [4].

The following components were chosen for the High-Tech Fidget Spinner controller board from the requirements discussed previously:

- **Microcontroller:** Teensy 4.1 due to its plethora of assignable GPIO for UART, I2C and SPI, and a built-in MicroSD card slot [15].
- **Stepper motor driver:** TMC2209 due to its SpreadCycle chopper and 256 microstepping resolution [27].
- **Rotary encoder:** E38S6G5-100B-G24N optical rotary encoder.

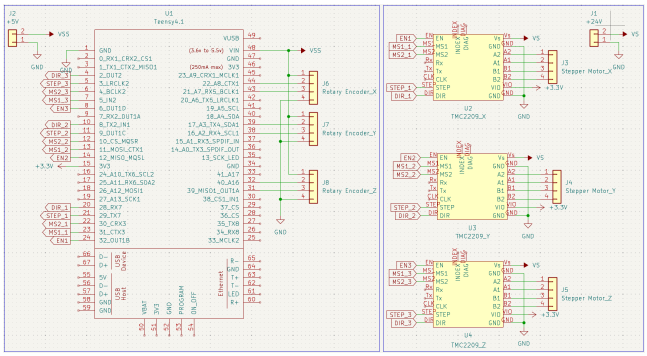

Figure 8: Schematic of the controller for the High-Tech Fidget Spinner.

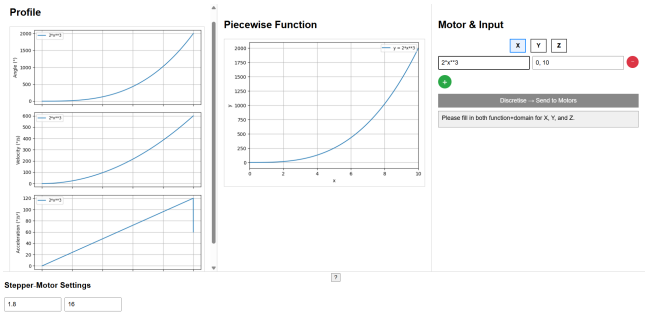

Figure 9: Web app with input fields and discretisation (right), and visual trajectories (centre and left).

5.2 Schematic

Figure 8 shows the controller schematic consisting of a Teensy 4.1 microcontroller, three TMC2209 drivers and generic pin connectors to the stepper motors and rotary encoders.

The PCB layout is available on GitHub alongside the KiCad 9.0 project files. To reproduce the project, the controller board can also be constructed on a breadboard. An external power supply ($\geq 120W$) is required to supply $+24V$ and $+5V$.

5.3 Code Explanation

The web app GUI shown in Figure 9 allows the user to:

- Adjust their stepper motor parameters.
- Enter a trajectory as a piecewise function for each axis of rotation.
- Swap between the axes of rotation.
- Plot the trajectory entered.
- Discretise and save the trajectories onto a MicroSD card once all of them have been entered.

Figure 10 shows the change between processes due to user inputs. The user can define bespoke trajectories as continuous piecewise functions. The mathematics used to discretise them into executable stepper motor trajectories is as follows:

5.3.1 User Input and Function Parsing. Each motor axis $M \in \{X, Y, Z\}$ accepts a piecewise-defined angular trajectory as a set of symbolic

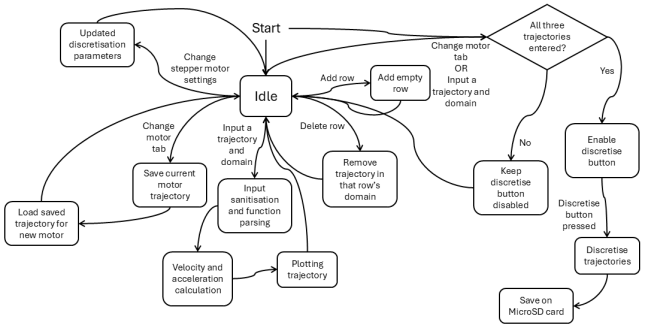

Figure 10: Web application interaction flow diagram.

functions $f_i(t)$ defined over domains $[a_i, b_i]$. These functions are parsed and converted into numerical callables using symbolic mathematics:

$$f_i(t) = \text{sympify}(\text{user input}), \quad f_i^{\text{num}}(t) = \text{lambdify}(f_i(t), \text{numpy}) \tag{1}$$

5.3.2 Angular Resolution and Discretisation Step Size. The system computes the angular resolution per microstep:

$$\theta_{\text{res}} = \frac{\theta_{\text{step}}}{\mu} \tag{2}$$

where θ_{step} is the step angle (in degrees) and μ is the number of microsteps.

The angular trajectory is initially sampled at 1,000 uniform time points to compute the maximum angular velocity via first-order finite differences:

$$v_{\max} = \max \left| \frac{d\theta}{dt} \right| \approx \max_j \left| \frac{\theta_{j+1} - \theta_j}{t_{j+1} - t_j} \right| \tag{3}$$

The discretisation time step dt is then computed as:

$$dt = \max \left(\frac{\theta_{\text{res}}}{v_{\max}}, \; dt_{\min} \right) \tag{4}$$

where $dt_{\min}$ is a fixed lower bound to prevent oversampling (e.g., $dt_{\min} = 0.002$ s).

5.3.3 Sampling and Trajectory Construction. For each segment $f_i^{\text{num}} \in [a_i, b_i]$, we compute the number of samples:

$$N_i = \left\lceil \frac{b_i - a_i}{dt} \right\rceil + 1 \tag{5}$$

The time samples are then uniformly spaced:

$$t_j \in \text{linspace}(a_i, b_i, N_i), \quad \theta_j = f_i^{\text{num}}(t_j) \tag{6}$$

The full trajectory is constructed by concatenating all segments while avoiding duplicate boundary points.

5.3.4 Velocity and Acceleration Profiling. Given the discretised angular positions θ_j, the velocity and acceleration profiles are computed numerically via finite differences:

$$\omega_j = \frac{\theta_{j+1} - \theta_j}{dt} \tag{7}$$

$$\alpha_j = \frac{\omega_{j+1} - \omega_j}{dt} \tag{8}$$

These profiles are plotted and visualised for motion quality analysis.

5.3.5 Validation and Export. The discretisation process is only enabled once valid input functions and domains are defined for all three axes X, Y, Z. Upon triggering, the discretised trajectories are stored as interleaved binary sequences:

$$[\text{uint32 } N][\text{float32 } t_0, \theta_0, t_1, \theta_1, \ldots, t_{N-1}, \theta_{N-1}] \tag{9}$$

These files are written to an SD card and interpreted by a microcontroller for real-time motor control.

6 Evaluation and Benchmarking

6.1 Method

Infrared reflectors were placed on the High-Tech Fidget Spinner. An Optitrak Prime X 22 motion capture system was used to capture its motion while performing a step trajectory from 0° to 90° in increments of 10°.

6.2 Results

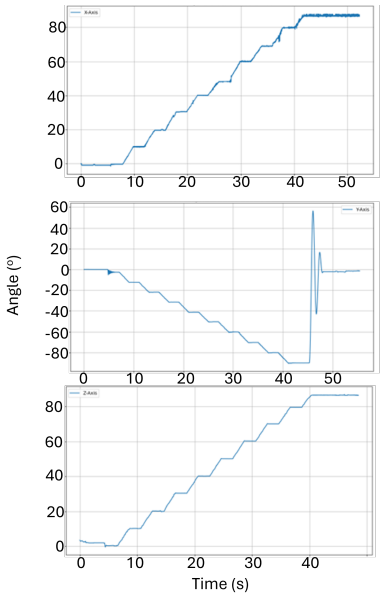

Figure 11: Euler angles of the X-axis (top), Y-axis (middle) and Z-axis (bottom) rotation.

Figure 11 plots X-axis rotation under the stepped trajectory, where non-zero start and end velocities cause oscillatory motion and an increasing range over time.

The Y-axis is plotted from 0° to −90°, per the defined rotation direction relative to the motion capture coordinate system. It ends with a large oscillation due to a manual Y-axis reset.

The Z-axis follows a similar trend as the X-axis, but with a smaller range over time. This is due to a smaller oscillation amplitude about the Z-axis as the bodies rotating about it have a larger moment of inertia due to a greater cumulative mass.

Table 2 gives summary statistics for the errors:

Table 2: Error analysis

	X-axis	Y-axis	Z-axis
Smallest mean deviation / °	-0.075	0.08	0.18
Largest mean deviation / °	-0.87	1.17	0.34
Smallest range / °	0.01	0.008	0.04
Largest range / °	1.4	5.2	2.3

6.3 Discussion

There were random errors present in the experiment, as the infrared reflectors were manually placed and stuck on using tape. Due to this, there are random errors in marker alignment and since the tape did not create a perfectly rigid joint, the markers underwent harmonic oscillations during acceleration which is shown by the data plotted in Figure 11.

The trajectory chosen was a step trajectory with a linear ramp between each step. This leads to a non-zero starting and ending velocity, and hence, jerky motion. The largest ranges were observed during harmonic oscillation when the High-Tech Fidget Spinner first started moving upon being powered on. The jerky motion due to the trajectory coupled with the stepper motors jumping to their nearest full steps, are likely reasons behind the largest ranges being one to two orders of magnitude larger than the smallest ranges.

6.4 Future Work

To address the jerky motion issue, it would be beneficial to explore what effect higher-order polynomial trajectories [18] have on a low-cost and open-source IMU calibration turntable. A closed-loop control system for the stepper motors, such as PID control, remains to be explored for more accurate motions [8].

7 Conclusion

Combining 3D-printed components, off-the-shelf 3D printer hardware, and open-source firmware, the artifact achieves 0.075° mean deviation with 0.008° range (Table 2) - within an order of magnitude of commercial systems like the Firepower Control 2TS-450 (Table 1), while remaining fully findable, accessible, interoperable, and reproducible. This unprecedented, high-precision design democratises advanced IMU testing — all for under £500.

References

[1] Jacob S Arlotti, William O Carroll, Youness Afifi, Purva Talegaonkar, Luciano Albuquerque, John E Ball, Harish Chander, Adam Petway, et al. 2022. Benefits of IMU-based wearables in sports medicine: Narrative review. *International Journal of Kinesiology and Sports Science* 10, 1 (2022), 36–43.

[2] Michelle Barker, Neil P Chue Hong, Daniel S Katz, Anna-Lena Lamprecht, Carlos Martinez-Ortiz, Fotis Psomopoulos, Jennifer Harrow, Leyla Jael Castro, Morane Gruenpeter, Paula Andrea Martinez, et al. 2022. Introducing the FAIR Principles for research software. *Scientific Data* 9, 1 (2022), 622.

[3] Firepower Control. 2025. Remote Control Position Rate Turntable For INS IMU Test And Calibration 2TS-450. https://www.accelerometergyro.com/sale-30377756-remote-control-position-rate-turntable-for-ins-imu-test-and-calibration.html. Accessed: 2025-07-09.
[4] Zhang Daniel. [n. d.]. What is the difference between incremental encoder's PPR, CPR and LPR? https://www.omc-stepperonline.com/support/what-is-the-difference-between-incremental-encoder-s-ppr-cpr-and-lpr. Accessed: 2025-07-09.
[5] Clarence W De Silva. 2004. *An Integrated Approach.* Boca Raton, FL: CRC Press.
[6] Analog Devices. 2020. Mastering Precision: Understanding Microstepping in Motion Control. *Analog Dialogue* (2020). https://www.analog.com/en/resources/analog-dialogue/articles/mastering-precision-understanding-microstepping.html Microstepping benefits and open-loop precision.
[7] Philipp Eisele, Sajid Nisar, and Franz Haas. 2024. A conceptual examination of an additive manufactured high-ratio coaxial gearbox. *Artificial Life and Robotics* 29, 3 (2024), 416–422.
[8] Nehal M Elsodany, Sohair F Rezeka, and Noman A Maharem. 2011. Adaptive PID control of a stepper motor driving a flexible rotor. *Alexandria Engineering Journal* 50, 2 (2011), 127–136.
[9] Blue Equator. 2021. High-Precision Automated Dual-Axis Positioning Turntable for INS & IMU Calibration. https://blueequator-ai.com/products/high-precision-automated-dual-axis-positioning-turntable-for-optical-measurement,-aerospace,-and-robotics-calibration. Accessed: 2025-07-09.
[10] Sina Gholamian and Paul AS Ward. 2021. A comprehensive survey of logging in software: From logging statements automation to log mining and analysis. *arXiv preprint arXiv:2110.12489* (2021).
[11] Handy_Bear. 2022. How to Make a Motorized Lazy Susan With a Secret. https://www.instructables.com/How-to-Make-a-Motorized-Lazy-Susan-With-a-Secret/. Accessed: 2025-07-09.
[12] iMAR Navigation & Control. 2017. iMAR iTURN-3S1. https://www.imar-navigation.de/downloads/TURN-3S1.pdf. Accessed: 2025-07-09.
[13] iMAR Navigation & Control. 2024. iMAR iTURN-2D1-HIL. https://www.imar-navigation.de/downloads/TURN-2.pdf. Accessed: 2025-07-09.
[14] iMAR Navigation & Control. 2025. iTES-PDT-07. https://www.imar-navigation.de/downloads/TES_PDT07_turntable.pdf. Accessed: 2025-07-09.
[15] Adafruit Industries. [n. d.]. PJRC Teensy 4.1 Development Board. https://mm.digikey.com/Volume0/opasdata/d220001/medias/docus/425/4622_Web.pdf. Accessed: 2025-07-09.
[16] JAYEGT. 2020. JAYEGT Motorized Rotating Display Stand, 7.87inch /17.6lbs Load, 360 Degree Electric Rotating Turntable for Photography Products, Jewelry, Cake,3D Model ,Mirror Cover (White). https://www.amazon.co.uk/JAYEGT-Motorized-Rotating-Turntable-Photography/dp/B08QS6YTHK. Accessed: 2025-07-09.
[17] Hua-Kun Jia, Lian-Dong Yu, Hui-Ning Zhao, and Yi-Zhou Jiang. 2019. A new method of angle measurement error analysis of rotary encoders. *Applied Sciences* 9, 16 (2019), 3415.
[18] Hossein Barghi Jond, Vasif V Nabiyev, and Rifat Benveniste. 2016. Trajectory planning using high order polynomials under acceleration constraint. *Journal of Optimization in Industrial Engineering* 10, 21 (2016), 1–6.
[19] Min Jung Kang and Yong Cheol Hwang. 2022. Exploring the factors affecting the continued usage intention of IoT-based healthcare wearable devices using the TAM model. *Sustainability* 14, 19 (2022), 12492.
[20] Alberto Leardini, Lorenzo Chiari, Ugo Della Croce, and Aurelio Cappozzo. 2005. Human movement analysis using stereophotogrammetry: Part 3. Soft tissue artifact assessment and compensation. *Gait & posture* 21, 2 (2005), 212–225.
[21] Isaac Lara Mekre Mesganaw. 2022. Differences Between Optical and Magnetic Incremental Encoders. https://www.ti.com/lit/ab/slya061/slya061.pdf?ts=175271104591. Accessed: 2025-07-09.
[22] MertArduino. 2025. How to Build a Motorized 3D Scanning Turntable for Your Phone. https://www.instructables.com/How-to-Build-a-Motorized-3D-Scanning-Turntable-for/. Accessed: 2025-07-09.
[23] RepRap. 2015. Backlash. https://reprap.org/wiki/Backlash. Accessed: 2025-07-09.
[24] Ltd. Shenzhen Huofeng Technology Co. 2014. Three-Axis Turntable with Thermal Control for IMU Gyro Accelerometer Sensor. https://shenzhenhuofeng.en.made-in-china.com/product/kfoRCbMGkwWN/China-Three-Axis-Turntable-with-Thermal-Control-for-Imu-Gyro-Accelerometer-Sensor.html. Accessed: 2025-07-09.
[25] Ltd. Shenzhen Huofeng Technology Co. 2024. Single-Axis Rotary Rate Position Turntable for Imu Gyro Calibration with Thermal Chamber. https://shenzhenhuofeng.en.made-in-china.com/product/rZKGcOSWwMtd/China-Single-Axis-Rotary-Rate-Position-Turntable-for-Imu-Gyro-Calibration-with-Thermal-Chamber.html?pv_id=1ivd6vdqb9d2&faw_id=1ivd6veb0bc3&bv_id=1ivd704253ac&pbv_id=1ivd6vbrf001. Accessed: 2025-07-09.
[26] Downeast Thunder. 2020. DIY Motorized Turntable (FREE PLANS!). https://www.homemadetools.net/forum/diy-motorized-turntable-free-plans-82676. Accessed: 2025-07-09.
[27] Trinamic. 2023. TMC2209 Datasheet. https://www.analog.com/media/en/technical-documentation/data-sheets/tmc2209_datasheet_rev1.09.pdf. Accessed: 2025-07-09.
[28] Eduardo Minuzzi Viera, William D'Andrea Fonseca, and Álysson Raniere Seidel. [n. d.]. Development of a Turntable for Multidisciplinary Teaching Applications in Electrical, Electronical, and Acoustical Engineering. ([n. d.]).
[29] Jan P Vox, Anika Weber, Karen Insa Wolf, Krzysztof Izdebski, Thomas Schüler, Peter König, Frank Wallhoff, and Daniel Friemert. 2021. An evaluation of motion trackers with virtual reality sensor technology in comparison to a marker-based motion capture system based on joint angles for ergonomic risk assessment. *Sensors* 21, 9 (2021), 3145.
[30] Sohrob Milani Zadeh, Joy MacDermid, James Johnson, Trevor B Birmingham, and Erfan Shafiee. 2023. Applications of wearable sensors in upper extremity MSK conditions: a scoping review. *Journal of NeuroEngineering and Rehabilitation* 20, 1 (2023), 158.

Received 20 February 2007; revised 12 March 2009; accepted 5 June 2009